Korean Journal of Geomatics
Vol. 3, No. 2 / March 2004
pp. 129~140

Cycle Slip Detection and Ambiguity Resolution for High Accuracy of an Integrated GPS/Pseudolite/INS System

Woon-Young PARK*, Hung-Kyu LEE and Jae-One LEE*****

Abstract

This paper addresses solutions to the challenges of carrier phase integer ambiguity resolution and cycle slip detection/identification, for maintaining high accuracy of an integrated GPS/Pseudolite/INS system. Such a hybrid positioning and navigation system is an augmentation of standard GPS/INS systems in localized areas. To achieve the goal of high accuracy, the carrier phase measurements with correctly estimated integer ambiguities must be utilized to update the system integration filter's states. The occurrence of a cycle slip that is undetected is, however, can significantly degrade the filter's performance. This contribution presents an effective approach to increase the reliability and speed of integer ambiguity resolution through using pseudolite and INS measurements, with special emphasis on reducing the ambiguity search space. In addition, an algorithm which can effectively detect and correct the cycle slips is described as well. The algorithm utilizes additional position information provided by the INS, and applies a statistical technique known as the cumulative-sum (CUSUM) test that is very sensitive to abrupt changes of mean values. Results of simulation studies and field tests indicate that the algorithms are performed pretty well, so that the accuracy and performance of the integrated system can be maintained, even if cycle slips exist in the raw GPS measurements.

Keywords : *GPS/Pseudolite/INS Integration, Carrier phase, Ambiguity Resolution, Cycle Slip*

1. Introduction

An integrated GPS/Pseudolite/INS system has been proposed and developed to overcome some drawbacks of existing kinematic positioning and navigation systems (Lee, 2002, Lee et al., 2002). This system can be basically implemented with three different GPS/ Pseudolite measurements, such as Doppler, pseudo-range, and carrier phase. In order to obtain high-accuracy results with such a system, the carrier phase observation has to be used in the system filter update. It is, however, prerequisite for the integer ambiguities to be resolved before the carrier phase measurements can be utilized in the filter update. These ambiguities remain constants as far as no loss of - signal lock occurs. In the event of signal loss, the integer counter is reinitialized, causing a jump in the instantaneous accumulated phase by an integer number of cycles. Such a jump is called a 'cycle slip', and corrupts the carrier phase measurement, resulting in the integer ambiguity value to be different after the cycle slip, compared with its value before the slip. Hence, it must be 'repaired' before the phase data is processed as double-differenced (DD) observations. On the other hand, ambiguity resolution (AR) is the mathematical process of converting ambiguous ranges (integrated carrier phase) to unambiguous ranges of millimetre measurement precision (Rizos, 1999). The AR process consists of two particular steps, such as the 'ambiguity estimation', and the 'ambiguity validation'. Whilst the former is a step to find the least-squares estimates of the integer ambiguities, the later is a part regarding

*Member, Professor, School of Ocean and Civil Engineering, Dong-A University, Busan, Korea (E-mail : uypark@mail.donga.ac.kr)
**Member, PhD Candidate, School of Surveying and Spatial Information Systems, The University of New South Wales, Sydney, Australia (E-mail : hung.lee@student.unsw.edu.au)
***Member, Senior Researcher, Korea Association of Surveying & Mapping (E-mail : jolee@kasm.or.kr)

The manuscript for this paper was submitted for review on January 12, 2004 / accepted on March 17, 2004

the question whether one is willing to accept this integer least-squares solution. It is well known that AR on-the-fly for short-range kinematic position can be readily resolved with dual-frequency measurements and assumption that the orbit bias and differential ionospheric delay can be ignored. However, for single-frequency based approach, it is still challenge to fast resolve the ambiguities (Han, 1997; Wang et al., 2003).

In this contribution, an AR procedure cooperated with pseudolite signals and INS will be described for the single frequency AR. This approach is expected to make it possible to quickly resolve the ambiguity through improving the float ambiguity precision and decorrelating the ambiguities. A more realistic stochastic modelling and a statistically rigorous ambiguity validation test scheme are also adapted to enhance the quality of ambiguity resolution. On the other hand, a cycle slip detection and identification algorithm, which can be easily implemented in the integration system, will be addressed. The algorithm uses the GPS antenna position provided by the INS to calculate cycle slip decision values, and applies the cumulative-sum (CUSUM) test to small persistent changes in the mean and/or standard deviation of the measurements (Mertikas and Rizos, 1997; Metikas, 2001). Finally, both simulation and field test results will be presented to manifest the performance of the proposed algorithms.

2. On-The-Fly Ambiguity Resolution

This section describes a scheme for integer ambiguity estimation based on double-differenced GPS/Pseudolite carrier phase and pseudo-range measurements from a single-frequency receiver, and an Inertial Navigation System (INS).

2.1 Observation equation

Linearization of the DD GPS/pseudolite observation equation with the INS-predicted antenna position can be expressed as the following Gauss-Markov model:

$$L = AX + V \tag{1}$$

where L is the measurement vector, A is the design matrix, and V is the residual vector:

$$A = \begin{bmatrix} A_b & \lambda I_{m\times m} \\ A_b & 0_{m\times m} \\ I_{3\times 3} & 0_{3\times m} \end{bmatrix} \tag{2a}$$

$$X = \begin{bmatrix} X_b \\ X_a \end{bmatrix} \tag{2b}$$

$$L = \begin{bmatrix} \nabla\Delta\phi - \nabla\Delta\rho_0 \\ \nabla\Delta R - \nabla\Delta\rho_0 \\ r_{i-1}(+) + \Delta r - r_0 \end{bmatrix} \tag{2c}$$

where λ is the carrier phase wavelength, A_b is the $m\times 3$ DD design matrix that contains information on the relative receiver-satellite geometry, X_b is the 3-vector of the unknown increments of the three-dimensional baseline components, and X_a is the m-vector of the real-valued unknown DD integer ambiguities. $\nabla\Delta\phi$, $\nabla\Delta R$, and $\nabla\Delta\rho_0$ are the m-vector of the DD GPS/pseudolite carrier phase, pseudo-range measurements, and the DD geometric distance, respectively (computed with respect to an approximate antenna position r_0). $r_{i-1}(+)$ is the filter-updated position at $i\text{-}1_{st}$ epoch, and Δr is the position increments obtained from INS mechanization between two consecutive epochs (e.g, Farrell & Barth, 1998, Savage, 2000)

A corresponding covariance matrix for the observation equation can be written:

$$Q_l = \sigma_0^2 \begin{bmatrix} Q_{\nabla\Delta\phi} & 0 & 0 \\ 0 & Q_{\nabla\Delta R} & 0 \\ 0 & 0 & Q_{\Delta r} \end{bmatrix} \tag{3}$$

where $Q_{\nabla\Delta\phi}$ and $Q_{\nabla\Delta R}$ is the $m\times m$ cofactor matrix for the DD GPS/pseudolite carrier phase and pseudo-range observations respectively, and $Q_{\Delta r}$ is the 3×3 cofactor matrix for the INS positioning solution, which is obtained from the position component of the co variance matrix $Q_{i_{GPS/INS}}(-)$ of the predicted states as follows (Lee, 2002, Lee et al., 2002):

$$Q_{i_{GPS/INS}}(-) = \Phi_{i,i-1} Q_{i-1_{GPS/INS}}(+) \Phi_{i,i-1}^{T} + R_{i-1} \tag{4}$$

where $\Phi_{i,i-1}$ is the Kalman filter transition matrix, $Q_{i-1\,GPS/INS}(+)$ is the Kalman filter-updated covariance matrix at $i\text{-}1_{st}$ epoch, and $R_{i\text{-}1}$ is the system noise matrix.

Stochastic modelling, which determines the values of equation (3), is a crucial step for AR. Q_{ins} matrix can be obtained from the system integration filter (e.g. equation (4)). An on-line stochastic estimation scheme for GPS and pseudolite (PL) observations based on post-fit residuals is adapted in this procedure to determine $Q_{\nabla\Delta R}$ and $Q_{\nabla\Delta\phi}$. A realistic covariance matrix for the observations can be estimated based on

the residual series from previous epochs as follows (Wang, 1999):

$$Q_{\nabla\Delta\phi,R} = Q_{\hat{V}_{GPS/PL}} + A_{GPS/PL} Q_{\hat{X}} A_{GPS/PL}^T = \frac{1}{N}\sum_{i=1}^{N} \hat{V}_{i-k}\hat{V}_{i-k} + A_{GPS/PL} Q_{\hat{X}_i} A_{GPS/PL}^T \quad (5)$$

where $Q_{\hat{V}_{GPS/PL}}$ is the covariance matrix for the residuals of GPS/PL measurements, $A_{GPS/PL}$ is the design matrix that contains line-of-sight vectors for GPS/pseudolite, $Q_{\hat{X}}$ is the covariance matrix for the unknown parameters, i denotes the current epoch, and N is the width of the moving data 'window' (ibid).

Special attention should be paid to the selection of the window width. According to *ibid*, an optimal width of the window is in the range of 10-30 epochs with 1-second sampling rate. One of the main benefits of this approach is that it is unnecessary to separately model satellite and pseudolite measurements. Using the estimated covariance matrix for the observations, the precision of the estimation results can be improved, and therefore a better AR performance can be expected.

2.2 Integer ambiguity estimation

The least-squares principle is used to compute estimates for the baseline increments and the DD integer ambiguities:

$$V^T PV = \text{minmum, with } X_b \in R^3 \text{ and } X_a \in Z^m \quad (6)$$

where $P=Q_l^{-1}$, R^3 and Z^m refers to 3-dimensional real space and m-dimensional integer space.

The estimation is performed in two steps, such as real-valued (float) ambiguity and integer ambiguity.

Based on the criterion in equation (6), the estimates of the unknown parameters X in equation (1) can be obtained by:

$$\hat{X} = (A^T PA)^{-1} A^T PL, \quad (7)$$

$$Q_{\hat{X}} = (A^T PA)^{-1} = \begin{bmatrix} Q_{\hat{X}_b} & Q_{\hat{X}_b\hat{X}_a} \\ Q_{\hat{X}_a\hat{X}_b} & Q_{\hat{X}_a} \end{bmatrix} \quad (8)$$

$$V = L - A\hat{X} \quad (9)$$

$$\hat{s}_0^2 = \frac{\Omega_0}{m}, \quad (10)$$

with,

$$\Omega_0 = V^T PV = L^T PL - L^T PA\hat{X} \quad (11)$$

where $\hat{X} = (\hat{X}_b, \hat{X}_a)^T$; $\hat{X}_b$ and $\hat{X}_a$ is the baseline and the real-valued (float) ambiguity vector; $Q_{\hat{X}}$ is the cofactor matrix of the estimated unknown parameters; V is the least-squares residual vector; $\hat{s}_0^2$ is the *a posteriori* variance cofactor.

After estimating the float ambiguities, search for integer ambiguity combination that satisfies the following equation performs.

$$\left\|\hat{X}_a - x_a\right\|^2_{\hat{s}_0^2 Q_{\hat{X}_a}} = \min, \; x_a \in Z^m \quad (12)$$

This minimization provides the integer least-squares estimation for the vector of ambiguity $\breve{X}_a$.

For the searching, Least-squares AMBiguity Decorrelation Adjustment (LAMBDA) method (Teunissen, 1993; De Joge & Tiberius, 1996) is used in this procedure. The main feature of the method is the decorrelation of the ambiguities, so-called Z-transformation.

Finally, if the ambiguity elements $\hat{X}_a$ are fixed to the integer values $\breve{X}_a$, the fixed baseline solution can be obtained as follows:

$$\breve{X}_b = \hat{X}_b - Q_{\hat{X}_b\hat{X}_a} Q_{\hat{X}_a}^{-1} \left(\hat{X}_a - \breve{X}_a\right) \quad (13)$$

$$Q_{\breve{X}_b} = Q_{\hat{X}_b} - Q_{\hat{X}_b} Q_{\hat{X}_a}^{-1} Q_{\hat{X}_a\hat{X}_b} \quad (14)$$

and,

$$\breve{\Omega}_0 = \Omega_0 + \left(\hat{X}_a - \breve{X}_a\right)^T Q_{\hat{X}_a}^{-1} \left(\hat{X}_a - \breve{X}_a\right) \quad (15)$$

2.3 Ambiguity validation

When one or more integer ambiguity combinations are accepted, the integer ambiguity combination resulting in the minimum quadratic form of the least-squares residual (e.g., equation 15) will be considered as the most likely (best) solution. However, it is very crucial to ensure that the most likely integer ambiguity combination is statistically better than the second best combination as defined by the second minimum quadratic form of the least-squares residuals (*ambiguity validation test*).

The ambiguity validation test procedures have been based on F-ratio of the second minimum quadratic form of the least-squares residuals and the minimum quadratic form of the least-squares residuals (Counselman

and Abbot, 1989). However, such a test has a risk not to know its probability distribution. Hence, the validation test procedure suggested by Wang et al. (1998) is implemented in order to overcome the drawback of the validation test using the *F*-ratio. The procedure is based on the ratio (called *W*-ratio) of the difference between the minimum and second minimum quadratic forms of the least-squares residuals and its standard deviation. The *W*-ratio value can be defined as (ibid):

$$W = \frac{d}{s_0\sqrt{Q_d}} \tag{16}$$

where

$$d = \breve{\Omega}_{0(second)} - \breve{\Omega}_{0(first)} \tag{17}$$

$$Q_d = \left(\breve{X}_{a(second)} - \breve{X}_{a(first)}\right)^T Q_{\hat{X}_a}^{-1}\left(\breve{X}_{a(second)} - \breve{X}_{a(first)}\right) \tag{18}$$

where Q_d is the covariance of d, and s_0^2 is *a posteriori* variance. In this situation, the W-ratio has a Student's *t*-distribution. A critical value for the test statistics is determined by choice of test confidence level and redundancy.

2.4 Simulation studies

A series of intensive simulation analyses based on Ambiguity Dilution of Precision (ADOP), which represents both precision and correlation characteristics of the estimated ambiguities (Teunissen, 1997) were carried out to investigate some impacts of the inclusion of INS and Pseudolite in the AR. In the analyses, GPS satellite and pseudolite constellation was generated by a GNSS simulation tool (Lee et al., 2002), while covariance matrix for INS-predicted positions was obtained though covariance simulation (Farrell and Barth, 1998). Note that observable precision (1σ) of GPS and pseudolite pseudo-range and carrier phase is considered as 0.3m and 0.005m respectively, while INS to be considered is a tactical-trade (gyro drift 5 deg/h and accelerometer bias 500 μg).

The inclusion of the pseudolites will enhance the satellite geometry in that the number of measurements is increased and their line-of-sight vector between epoch changes by a large angle. Fig. 1 depicts ADOP changes for 30 second sequential solution as a function of the number of pseudolites used. Note that the INS-predected positions are included in the solutions. Overall results reveal the more pseudolte observations are used, the better AR performance is expected. However, it is of interesting that the ADOP is significantly decreased even though only one pseudolite is added to GPS constellation, but more than three pseudolites used does not improve the ADOP values much further. Another expected benefit with pseudolites in the AR is relatively quick change of line-of-singe vector that may more enhance the performance of the AR procedure because *satellite change geometry* plays crucial roles in this procedure. In order to investigate such an effect, three different user dynamics, which are accelerations of 0.1 m/sec^2, 0.5 m/sec^2, and 1.0 m/sec^2 respectively, are considered. It is important to be remembered that the line-of-sight is absolutely determined by the user's dynamic because the pseudolites are fixed on the ground. Fig. 2 illustrates that the vehicle dynamics effect in the AR due to the relatively large change of the pseudolite change geometry. Of course,

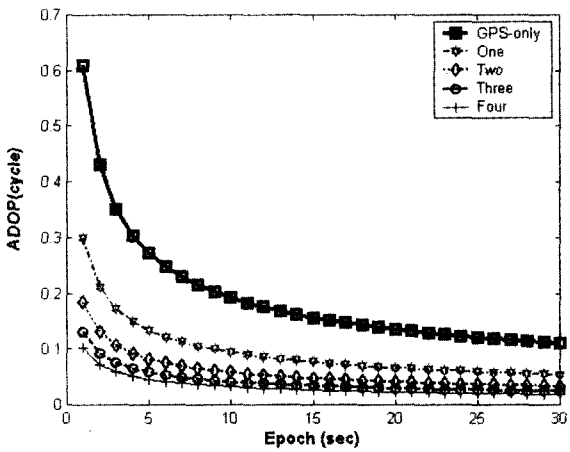

Fig. 1. Pseudolite effects in the AR (depending on the number of Pseudolites).

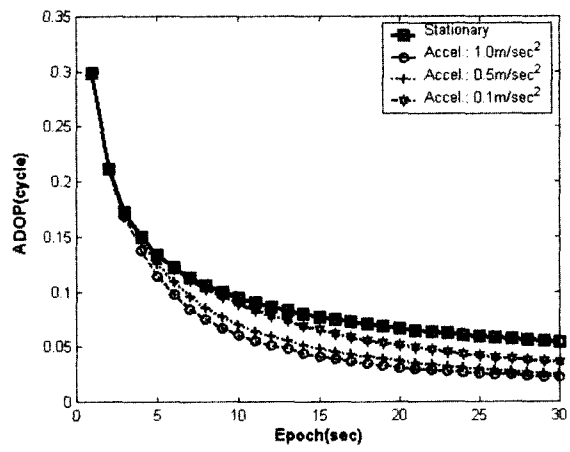

Fig. 2. Pseudolite effects in the AR (depending on the vehicle dynamics).

overall trend shows that the higher dynamics, the smaller ADOP values (more enhanced AR performance). However, the performance cannot be improved according to time (increased velocity). For instant, 0.5 m/sec and 1.0 m/sec acceleration cases becomes identical at the 30 second epoch, but on the other hand, the ADOP different is maximized around 10 second epoch. It may be caused by the fact that although the velocity is continuously increased, the user is getting far from the Pseudolie locations, and thus the relative change geometry becomes smaller.

More analyses were performed to probe the impacts of including INS-predicted position in the AR. However, an important fact to be considered is the length of the GPS/pseudolite signal blockage because an integration filter (Kalman) is unable to be updated, resulting in error growth of the INS-predicted position. The magnitude of the error depends on the length of the blockage, and influence in the resolution procedure. Moreover, during the resolution procedure, the filter cannot be updated by the accurate (ambiguity-fixed) carrier phase observation. Those facts will be considered in the analysis. Four different scenarios according to the blockage length are evaluated in the test (*instantaneous* (normally caused by cycle slip), 10 seconds, 20 seconds, and 30 seconds). Fig. 3 depicts the influence (ADOP) of introducing the INS-predicted position (and/or Pseudolites) in the AR as a function of the four different lengths of the signal outages. All the results in the case of both GPS/INS and GPS/PL/INS approach manifest the inclusion of INS significantly reduce the ADOP values, and hence better performance of the AR is expected. Looking into the results in more detail, we can also figure out the impacts of the different behaviour of INS-predicted position error. '*Instantaneous*' blockage (the smallest error growth) shows both GPS/INS and GPS/PL/INS approach with single frequency is indeed superior to that of dual frequency GPS-only case. In other words, it would be said that single epoch AR with such integration approach could be possible from this results. In the of the 10 second blockage, even though three results (Dual frequency GPS-only, GPS/INS, and GPS/PL/INS) are similar at the beginning, GPS/PL/INS and dual frequency results are getting close and much better than that of GPS/INS. Note that results from the dual frequency approach are always better than those of the integration approach after 20 and 30 second blockage. However, when considering epoch by epoch AR with dual frequency with respect to short base-line is possible, GPS/INS and GPS/PL/INS approach can resolve the ambiguity within a couple of seconds from those results. On the other hand, Fig. 4 illustrates the change of ADOP (AR performance) depending on the different length of the outage. It can be seen from the figure that the size of ADOP values is significantly different according to the magnitude of initial position errors, but those values are getting closer after 30 second sequential solution, which means time to fix ambiguities will be different (performance) with respect to the length of the signal blockage. However, the most impressive thing in the result is that aiding Pseudolite and INS would make it possible to significantly improve single frequency based AR.

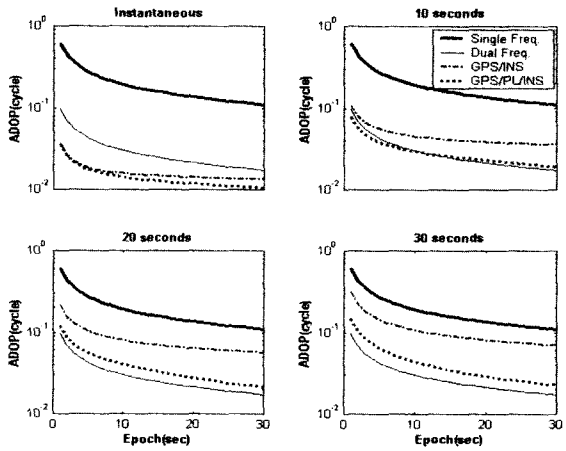

Fig. 3. Effects of including INS-predicted position in the AR, which compares GPS/INS and GPS/PL/INS system.

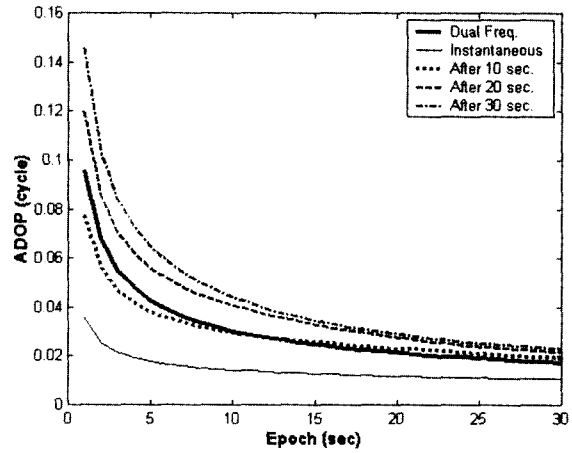

Fig. 4. Influences of INS-predicted position errors based on the GPS/PL/INS system in the AR.

3. Cycle slip detection and identification

3.1 Decision value and its statistical property

The basic task of the algorithm is to compare the DD GPS carrier phase observations $\nabla\Delta\phi^{GPS/PL}$ with the double-differenced geometric distances $\nabla\Delta\phi^{INS}$ computed using INS-predicted antenna positions. Let's define a decision value ($\delta\nabla\Delta\phi$) for short baseline (less than 15km) applications as follows:

$$\begin{aligned}\delta\nabla\Delta\phi &= \nabla\Delta\phi^{GPS/PL} - \nabla\Delta\phi^{INS} \\ &= \nabla\Delta N + \nabla\Delta m + \nabla\Delta\varepsilon^{GPS/PL} + \nabla\Delta\varepsilon^{INS}\end{aligned} \tag{19}$$

where $\nabla\Delta N$ is the DD integer ambiguity; $\nabla\Delta m$ is the DD multipath; $\nabla\Delta\varepsilon^{GPS/PL}$ is the remaining DD biases and measurement noise; $\nabla\Delta\varepsilon^{INS}$ is the DD geometric distance error caused by uncertainty of satellite and INS-predicted antenna positions.

The main error source in Equation (19) is multipath, although in this paper it is assumed that such a multipath error can be somehow modelled and/or mitigated by appropriate technologies. Hence the decision values can be written as follows (if the DD integer ambiguity is resolved at some previous epoch):

$$\delta\nabla\Delta\phi = \nabla\Delta\varepsilon^{GPS/PL} + \nabla\Delta\varepsilon^{INS} \tag{20}$$

Supposed that the residual systematic errors are ignored, the expected value of the measurement noise ($\nabla\Delta\varepsilon^{GPS/PL}$) would be:

$$E\left[\nabla\Delta\varepsilon^{GPS/PL}\right] \approx 0 \tag{21}$$

If two DD measurements are available, the covariance matrix is as follows (if homoscedastic and uncorrelated model is used):

$$cov\left[\nabla\Delta\varepsilon^{GPS/PL}\right] = 2\sigma^2\begin{bmatrix}2 & 1\\ 1 & 2\end{bmatrix} \tag{22}$$

Hence, the variance of one DD measurement is $4\cdot\sigma^2$ (Hofmann-Wellenhof *et al.*, 2001). Note that it can be different if another type of stochastic model is used.

If it is assumed that the satellite ephemeris errors are eliminated by double-differencing, the error ($\nabla\Delta\varepsilon^{INS}$) in equation (20) can be (Lee et al., 2003):

$$\nabla\Delta\varepsilon^{INS} = \underbrace{(a_X^i - a_X^j)}_{A_X}\delta x_M + \underbrace{(a_Y^i - a_Y^j)}_{A_Y}\delta y_M + \underbrace{(a_Z^i - a_Z^j)}_{A_Z}\delta z_M \tag{23}$$

with

$$A_X = \frac{x_{r0} - x_0^s}{\rho_0},\quad A_Y = \frac{y_{r0} - y_0^s}{\rho_0},\quad A_Z = \frac{z_{r0} - z_0^s}{\rho_0} \tag{24}$$

If the expected values of the integration's position error (X_{IP}) is zero with the assumption that the navigation parameters and sensor errors are reliably estimated (and corrected), and its covariance matrix can be obtained from the Kalman filter:

$$E(X_{IP}) = 0,\qquad Q_{IP} = \begin{bmatrix}\sigma_{xx} & \sigma_{xy} & \sigma_{xz}\\ \sigma_{yx} & \sigma_{yy} & \sigma_{yz}\\ \sigma_{xz} & \sigma_{yz} & \sigma_{zz}\end{bmatrix} \tag{25}$$

then the expected values of ($\nabla\Delta\varepsilon^{INS}$) are zero as well, if the remaining error sources are assumed eliminated by double-differencing. On the other hand, the covariance matrix can be derived using the covariance propagation law:

$$cov\left[\nabla\Delta\varepsilon^{INS}\right] = AQ_{IP}A^T \tag{26}$$

where

$$A = \begin{bmatrix}A_X^{aj} & A_Y^{aj} & A_Z^{aj}\\ A_X^{bj} & A_Y^{bj} & A_Z^{bj}\\ \vdots & \vdots & \vdots\\ A_X^{ij} & A_Y^{ij} & A_Z^{ij}\end{bmatrix} \tag{27}$$

Assuming that the GPS carrier phase measurements are uncorrelated in time, then the predicted position by INS and the actual carrier phase measurements are statistically uncorrelated since the predicted position is only affected by previous GPS/Pseudolite measurements. Thus the expected values of the decision values are (Altmayer, 2000, Lee et al., 2003):

$$E\left[\delta\nabla\Delta\phi\right] \approx 0 \tag{28}$$

and the variance can be obtained as follows:

$$\sigma^2\left[\delta\nabla\Delta\phi\right] = \sigma^2\left[\nabla\Delta\varepsilon^{GPS}\right] + \sigma^2\left[\nabla\Delta\varepsilon^{GPS}\right] \tag{29}$$

As a consequence cycle slip detection and identification can be carried out through continuously performing a hypothesis test with respect to the decision values under the aforementioned assumptions.

3.2 Cumulative-Sum test (Detection algorithm)

The decision values ($\delta\nabla\Delta\phi$) represent the cycle slip

indicating signals which makes possible not only the detection of slips, but also permits their magnitude to be determined. Assuming that the signal is characterised by a Gaussian distribution with the static properties described in the preceding section (see Equations 28 and 29), the CUSUM algorithm can be applied to detect the cycle slips.

The CUSUM algorithms can be classified into two types. The first type is the one-sided CUSUM, which can be used when both the means before and after the change are known. The second type is the two-sided CUSUM, to be used when the change magnitude is unknown. It is the two-sided CUSUM test that should be used for the cycle slip detection algorithm with a minimum detectable jump ($\delta\mu_{\min}$) because the expected slip size is unknown. This uses two CUSUM algorithms in parallel; the first one for detecting an increase in the mean, and the second for detecting a decrease in the mean of the sequence (Basseville, 1988; Basseville and Nikiforov, 1993). Thus, a slip will be detected if:

$$\begin{cases} g_n^* = s_n^* - \min\limits_{0\le t\le n} s_t^* \ge \lambda^* \\ g_n^* = \max\limits_{0\le t\le n} s_t^* - s_n^* \ge \lambda^* \end{cases} \tag{30}$$

where

$$s_t^* = s_{t-1}^* + \frac{\delta\mu_{\min}}{2\sigma^2}\left(x_t - \mu_0 - \frac{\delta\mu_{\min}}{2}\right), \quad s_0^* = s_0^* = 0 \tag{31}$$

To avoid the downward and upward drift of the CUSUM across and out of the page limits, an algebraic equivalent of equation (23) is used (Hawkins and Olwell, 1998; Mertikas, 2001):

$$\begin{cases} C_n^* = \max\left(0, C_{n-1}^* + g_n^*\right) \ge \lambda^* \\ C_n^* = \min\left(0, C_{n-1}^* + g_n^*\right) \ge \lambda^* \end{cases}, C_n^* = C_n^* = 0 \tag{32}$$

The resulting alarm time is given by:

$$t_a = \min\left\{t \ge 1 : (g_t^* \ge \lambda) \cup (g_t^* \ge \lambda)\right\} \tag{33}$$

In most cases very little is known about the change magnitude $\delta\mu_{\min}$. Three possible *a priori* choices can be made with respect to this parameter. The first is to choose $\delta\mu_{\min}$ as a minimum possible jump magnitude (limit case being $\delta\mu_{\min} = 0$). The second is to choose *a priori* the most likely jump magnitude. The third choice is a worst-case value from the point of view of the cost of missed detection(s). If the actual change in mean is less than that specified in the CUSUM test, then the single increments z_n of the log-likelihood ratio will always have a positive mean and the CUSUM scheme will be ineffective as a detector of change. It is common to specify a "rejectable level" $\delta\mu_{\min}$, then determine the threshold value λ so that the CUSUM test has a specified maximum rate of detection alarm with a minimum delay. A more detailed description of CUSUM parameter tuning is given in Hawkins and Olwell (1998) and Mertikas and Rizos (1997).

4. Field Test and Results

Land vehicle experiments were carried out on 23rd April 2003 at the Clovelly Bay Carpark in Sydney, Australia. The objective of these tests was to evaluate performance of the algorithms (e.g., AR and cycle slip detection) presented in the preceding sections.

4.1 General description of the tests

A prototype pseudolite system developed at UNSW was used in the experiments. The locations of the pseudolite and the reference station were precisely surveyed using Leica GPS system 500 receivers. During the trial the pseudolite signal was configured to transmit with the power of -10 dB (assigned PRN 12). Two Novatel Millennium receivers with Leica AT504 choke-ring antennas were used at both the reference and rover (vehicle) stations to track the GPS and pseudolite signals. The INS used in this experiment was a Boeing C-MIGITS II, which is considered to be a tactical-grade accuracy unit (5 deg/h, 500 μg). The antenna and INS were mounted on the roof of the test vehicle, as shown in Fig. 5. Raw INS sensor measurements (accelerations and angular velocities) were recorded at 100Hz, while the single-frequency GPS/pseudolite data were logged

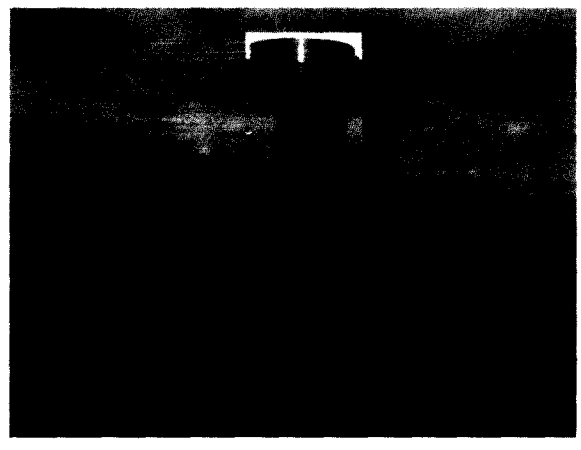

Fig. 5. Experiment set-up.

at 1Hz. During the experiment, there were 6 visible satellites (above the cut-off angle of 15°) and one pseudolite (PRN 12). The maximum baseline length between the reference station and the rover was of the order of 50 metres.

4.2 AR performance analysis

In order to demonstrate the performance of the presented AR procedure, a comparison between different system configurations was conducted. Three different configurations (GPS-only, GPS/INS, and GPS/pseudolite /INS) were applied for all the data processing in single-epoch solution mode. The AR performance can be evaluated by the comparison of ambiguity validation test statistics (W-ratio) obtained by equation (16), in that the larger values for the statistics the higher the probability of correctly fixing the integer ambiguity (Wang, 1999; Wang et al., 2003).

Table 1 shows ambiguity validation test results for different system configurations. It can be seen from the table that the *W*-ratio values in the case of using only GPS data, they are mostly less than their critical values (4.5 with 99% confidence level). This implies that most of the integer ambiguity combinations cannot be successfully validated. However, the ratios obtained by either integrated GPS/INS or GPS/pseudolite/INS are sufficiently large to validate the correct ambiguity for critical values (3.2 and 3.0 with 99.9% confidence level respectively). Comparing the results from the GPS/INS case with the GPS/pseudolite/INS case, it is revealed that the averaged ratio from the latter is slightly larger than that obtained from the former. Therefore the inclusion of pseudolite observations enhances the AR performance. In addition, the successful validation rates in the table for the three different system configurations based on the aforementioned critical values are 0.4%, 97.4%, and 99.3%, respectively. Hence it has been demonstrated that the proposed procedure based on GPS/Pseudolite/INS integration does indeed perform better.

A realistic estimation of measurement covariance matrices provides reliable statistics for AR. In order to clearly demonstrate this fact, the solutions based on the two different types of stochastic model, namely the 'Preset' and 'Estimated', are obtained. The 'Preset' model is based on a priori assumption of the measurement precision. For the 'Estimated' model, a realistic measurement covariance matrix is estimated using equation (5). Table 2 shows the validation test statistic (averaged *W*-ratio) and ambiguity successful validation rates according to the two stochastic models, indicating that the ambiguity validation test statistics with the 'Estimated' measurement covariance matrices are better than those with the 'Preset' measurement covariance matrices (see averaged *W*-ratio values). On the other hand, the successful validation rates for the 'Estimated' and 'Preset' are 92.1% and 99.3%, respectively, which demonstrates the AR performance with 'Estimated' model is superior to that of the 'Preset' models.

The capability of the integrated system to recover from complete GPS/pseudolite signal blockages, and return to a positioning solution with correctly resolved ambiguities, is critical to maintaining high system performance. Therefore the impact of including pseudolite and INS observations on the AR performance after complete GPS/pseudolites signal blockage was also investigated. For this test, signal blockages of 2, 5, 10, 20, 30, 40, and 50 seconds with respect to three different locations in the observation files (referred to as Case I, II, and III) are simulated through modifying the RINEX data files. Note that DD pseudo-range

Table 1. Ambiguity validation test results for different system configurations.

System Configuration	Averaged W-ratio values	Num. Of Validated Ambiguity combinations	Num. Of Not Validated Ambiguity Combinations	Validation Rate (%)
GPS-only	0.6	5	1395	0.4
GPS/INS	11.4	1363	37	97.4
GPS/PL/INS	15.2	1390	10	99.3

Table 2. Ambiguity validation test result for different stochastic model.

System Configuration	Averaged W-ratio values	Num. Of Validated Ambiguity combinations	Num. Of Not Validated Ambiguity Combinations	Validation Rate (%)
Preset	11.4	1289	111	92.1
Estimated	15.2	1390	10	99.3

measurements are used in the filter update for the AR procedure, and a sequential solution is applied to estimate the initial float ambiguities.

Table 3 shows the time-to-fix of L1 carrier phase ambiguities after complete GPS/pseudolite signal blockages. The results indicate that the AR performances of both GPS/INS and GPS/PL/INS are similar after a short signal outage (up to 10 seconds). However, the AR performance is significantly improved by including PL measurements from 20 second outage, excepting for 30 second blockage for Case III. Special attention should be paid to 'Case I', because the most significant improvement was obtained. Hence, it is demonstrated from the results that the proposed AR procedure based on GPS/pseudolite/INS integration makes it possible to resolve the ambiguities within a couple of seconds if the outage is relatively short. Moreover, the AR performance can be considerably enhanced even in the case of a blockage of 50 seconds. The different performances among the three cases appears to be caused by the different error growth rates of the INS-predicted positions, satellite geometry and/or measurement errors.

4.3 Cycle slip detection and identification tests

First of all, CUSUM tuning parameters were set, 0.5 cycles (approximate 9cm) and 0.4 for the minimum detectable value ($\delta\mu_{\min}$) and the threshold (λ) respec tively according to the CUSUM parameter tuning procedure proposed by Mertikas and Rizos (1997). A pre-processing was carried out to get the truth before analyzing the algorithm performance. A method use in this research was to examine DD carrier phase residuals computed with respect to antenna positions obtained from dual frequency GPS-only positioning. Note that such a data processing scheme provides a few centimeter level accuracy as long as the carrier phase ambiguities are resolved correctly (Rizos, 1996). The results revealed no cycle slip exists in all the GPS carrier phase observations, while thirteen slips could be identified in pseudlite measurements. Hence, it should be highlighted from the results that the pseudolite signal is tenderer against the slip than that of the satellite. It seems to be mainly caused by low pseudolite elevation angle and some obstructions in this test. For analyzing purpose, cycle slips were simulated into one of satellites

Table 3. Time to fix L1 carrier phase ambiguity after the different length of blockages.

Case	Outage Duration (Sec)	Time to fix ambiguities (sec)		
		GPS-only	GPS/INS	GPS/PL/INS
Case I	2	61	1	1
	5		5	5
	10		10	8
	20		20	14
	30		31	22
	40		36	20
	50		43	24
Case II	2	34	1	1
	5		1	1
	10		1	1
	20		5	2
	30		10	8
	40		16	11
	50		20	13
Case III	2	32	1	1
	5		3	1
	10		5	4
	20		6	4
	30		8	8
	40		15	8
	50		19	10

(SV 7) by editing Rinex observation file, which means the simulated ones were considered as the truth. On the other hand, the identified cycle slips of pseudolite (PL12) were used to the truth. Fig. 6 and 7 illustrate decision values and two-sided CUSUM values of SV 7 and PL 12 to give a closer insight into how the algorithm was performing during data processing. The top graphs in there figures depict the decision values with imposed cycle slips in raw measurements. The second and third show CUSUM values are kept as zero when no cycle slip occurs. At the presence of cycle slip, the detection threshold is exceeded and the cycle slip determination process identifies the affected double-differenced observations. Table 4 shows locations and magnitudes of the truth and ones identified from the proposed procedure. It is clearly seen from the results that the algorithm performs very well in that the slipped carrier phase measurements are successfully detected and identified without missing any slip even though some of the slips occur at two successive epochs.

5. Conclusions

Ambiguity resolution and cycle slip detection/identification are the most crucial steps in achieving high accuracy positioning results using an integrated GPS/Pseudolite/INS system. Hence, an ambiguity resolution procedure, which collaboratively uses GPS, pseudolite and inertial measurements, has been presented in this paper, aiming to improve the performance of a single-frequency on-the-fly AR. In the procedure, realistic stochastic modeling and statistically rigorous ambiguity validation scheme are adapted to enhance the reliability of ambiguity resolution. In addition to the ambiguity resolution, an effective cycle slip detection and identification scheme for single frequency observations has been addressed, which effectively makes

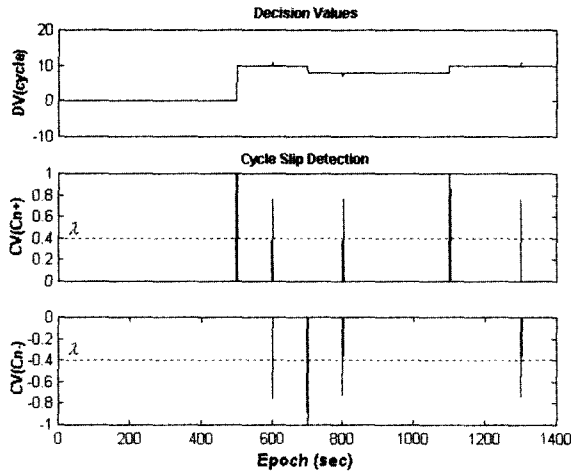

Fig. 6. CUSUM test for SV 7 (ref SV 4).

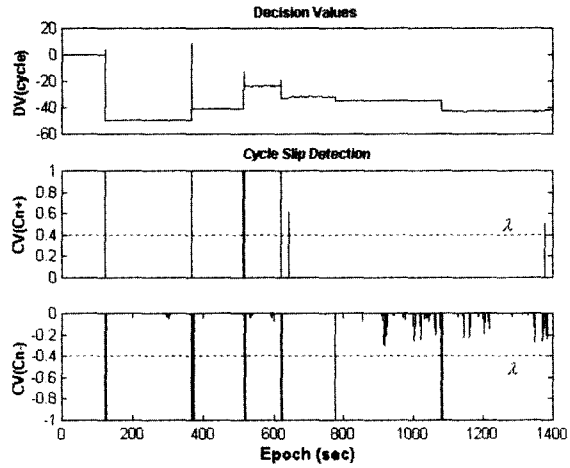

Fig. 7. CUSUM test for PL 12 (ref SV).

Table 4. Cycle Slip detection and identification procedure results.

Satellite PRN 09			Pseudolite PRN 12					
Epoch	Truth	Identified	Epoch	Truth	Identified	Epoch	Truth	Identified
500	+10	+10	123	+3	+3	644	+1	+1
600	+1	+1	124	-53	-53	776	-3	-3
601	-1	-1	368	+58	+58	1081	-8	-8
700	-2	-2	369	-48	-48	1307	+1	+1
800	-1	-1	374	-1	-1			
801	+1	+1	516	+28	+28			
1100	+2	+2	518	-11	-11			
1300	+1	+1	621	+5	+5			
1301	-1	-1	622	-14	-14			

use of the integrated GPS/Pseudolite/INS system. The algorithm employs additional GPS antenna positions provided by the INS navigation solutions, and the cumulative-sum (CUSUM) test is applied to detect the slips. Hence, it can be simply implemented in the system integration software.

Both simulation and field test results were conducted to appraise the performance of the proposed algorithms. From their results, the following conclusion could be drawn:

1. The INS predicted-position included in the ambiguity resolution can significantly improve the precision and correlation of float ambiguities (e.g., enhanced AR performance) as it reduces ADOP values.
2. The pseudolite measurements play an important role in the proposed AR procedure in that ADOP values can be largely decreased even if only *one* pseudolite is added to the GPS constellation. Furthermore, it is proved that the relatively rapid change of the line-of-sight vector enhances the performance of the AR process.
3. Stochastic modeling for the satellite and pseudolite measurements is critical to strengthen the AR performance, which means the more realistic model the better performance.
4. 'Instantaneous' resolution is feasible if the duration of the signal blockage is up to a couple of seconds. On the other hand, even if the signal blockage is up to 50 seconds, the ambiguities can be fixed within a few ten of seconds, depending on satellite/ pseudolite geometry and measurement precision.
5. Pseudolite signals are more vulnerable to cycle slips than those of the satellite due to the low pseudolite elevation angle and some obstructions. The cycle slips could be effectively detected and then instantaneously identified using the proposed algorithm even though the slips occurred at two successive epochs.

Acknowledgement

The second author (HKL) is supported in his PhD research by a Scholarship funded by the Kwanjeong Educational Foundation, Korea.

Reference

1. Altmayer, C. (2000). "Enhancing the integrity of integrated GPS/INS system by cycle slip detection and correction." *Proc. the IEEE intelligent Vehicles Symposium*, Dearborn, Miami, pp. 174-179.
2. Bassevile, M. (1998). "Detecting changes in signals and systems - a survey." *Automatica*, Vol. 24, No. 3, pp. 309-326.
3. Basseville, M. and Nikiforov, V. (1993). *Detection of Abrupt Changes - Theory and Applications*, Prentice Hall, New Jersey, 441pp.
4. Counselman, C.C. and Abbot, R. (1989). Method of Resolving Radio Phase Ambiguity in Satellite Orbit Determination, *J. Geophysical Research*, Vol. 94, pp. 7058-7064.
5. De Jonge, P.J., and Tiberius, C.C.J.M. (1996). *The LAMBDA method for integer ambiguity estimation : implementation aspects*, Delft Geodetic Computing Center LGR Series, no. 12, Delft University of Technology, 49pp.
6. Farrell, Ray A., and Barth, M. (1998). *The Global Positioning System & Inertial Navigation and Integration*, McGraw-Hill companies, Yew York, 340pp.
7. Han, S. (1997). *Carrier phase-Based Long-Range GPS Kinematic Positioning*, PhD Dissertation, School of Surveying and Spatial Information Systems, The University of New South Wales, Sydney, Australia, 185pp.
8. Hawkins, M.D and Olwell, D.H. (1998). *Cumulative Sum Charts and Charting for Quality Improvement* (Statistics for engineering and physical science), Berlin/Heidelberg: Springer Verlag, 247pp.
9. Hofmann-Wellenhof, Lichtenegger, B., H. and Collins, J. (2001) *GPS Theory and Practice*, 5th Edition, Springer-Verlag, Wien, 382pp.
10. Lee, H.K., Wang, J., Rizos, C., and Grejner-Brzezinska, D. (2002). "GPS/Pseudlite/INS integration : Concept and first tests." *GPS Solutions*, Vol. 6, No. 1-2, pp. 34-46.
11. Lee, H.K. (2002). "GPS/Pseudolite/SDINS integration approach for kinematic applications. *Proc. 15th Int. Tech. Meeting of the Satellite Division of the U.S. Inst. of Navigation*, Portland, Oregan, pp. 1464-1473.
12. Lee, H.K., Wang, J., Rizos, C., Li, B., and Park, W.Y. (2003). "Effective cycle slip detection and identification for high accuracy integrated GPS/INS positioning." *Proc. 6th Int. Symp. on Satellite Navigation Technology Including Mobile Positioning & Location Services*, Melbourne, Australia, CD-Rom Proc., paper 43.
13. Mertikas, S.P. (2001). "Automatic and on-line detection of small but persistent shifts in GPS station coordinates and statistical process control." *GPS Solutions*, Vol. 5, No. 1, pp. 39-50.
14. Mertikas, S.P., and Rizos C. (1997). "Online detection of abrupt changes in the carrier phase measurements of GPS", *J Geodesy*, Vol. 71, pp. 469-482.
15. Rizos, C. (1996). *Principles and Practice of GPS Surveying*, School of Surveying and Spatial Information Systems, The University of New South Wales, Sydney, Australia, 555pp.
16. Rizos, C., (1999). Quality issues in real-time GPS positioning, Final Report of the IAG SSG 1.154, (http://www.gmat.unsw.edu.au/ssg_RTQC/ssg_rtqc.pdf).
17. Savage, P.G. (2000). *Strapdown Analytics : Part I, Strapdown* Associates, Inc., 773pp.
18. Teunissen P.J.G. (1993). "A new method for fast carrier

phase ambiguity estimation." *Proc. IEEE Position, Location and navigation Symp.*: PLANS 94, Las Vegas, pp. 562-573.

19. Teunissen, P.J.G. (1997). "A canonical theory for short GPS baselines (Part I-IV)." *J. Geodesy*, Vol. 71, pp. 320-336, 389-401, 486-501, 513-525.
20. Wang J, Stewart, M.P., and Tsakiri, M. (1998). A discrimination test procedure for ambiguity resolution on-the-fly. *J. Geodesy*, Vol. 72, pp. 644-653.
21. Wang, J., Lee, H.K., Hewitson, S, Rizos, C., and Barnes, J. (2003). "Sensitivity analysis for GNSS integer carrier phase ambiguity validation test." *XXIIIth General Assembly of the IUGG*, Sapporo, Japan.